

# DEVELOPMENT OF A MULTI-POINT CHEST DEFLECTION MEASUREMENT SYSTEM FOR THE LARGE OMNIDIRECTIONAL CHILD (LODC) ANTHROPOMORPHIC TEST DEVICE (ATD)

**Mike Carlson**

**Brian Suntay**

Transportation Research Center Inc.  
USA

**Jason Stammen**

National Highway Traffic Safety Administration  
USA

Paper Number 23-0275

## ABSTRACT

**OBJECTIVE** The objective of this study is to evaluate the feasibility and accuracy of a multi-point chest deflection sensing system installed in the LODC using static, quasi-static, and two dynamic test conditions.

**METHOD** The multi-point LED chest deflection system was evaluated at four levels: (1) calibration verification, (2) quasi-static, (3) dynamic probe impact, and (4) dynamic drop tower in order to demonstrate that the sensor gave a reasonable and accurate measurement of chest deflection.

**RESULTS** Individual sensors were found to be quite accurate in static verification tests, and sensors installed in the LODC ribcage were also observed to match well with CMM measurements. In dynamic testing with the full array of sensors installed in the ribcage, LED deflection matched probe-measured deflection closely. In both frontal and oblique drop tower tests, individual sensor deflection time histories showed how the full array could capture full ribcage deformation.

**CONCLUSIONS** A novel non-contact sensor array to measure LODC chest deformation has been developed. This system has gone through a battery of both static and dynamic tests thus far to evaluate the system's performance. Initial results indicate that the system is promising for monitoring overall chest deformation in the LODC. Future work will include more dynamic testing to further understand how the system can describe three-dimensional ribcage deformation.

Keywords: LODC; chest deflection; multi-point; LED; testing

## INTRODUCTION

Thoracic injuries sustained by rear seated child occupants involved in vehicle crashes have been attributed to complex loading mechanisms including the belt and seatback [1]. Because children make up a large percentage of rear seated occupants [2], protection of the pediatric chest is critical. Historically, chest deflection has been the primary correlated measure to thorax injury risk when using anthropomorphic test devices (ATDs). It has also been hypothesized that thoracic injury in children is dependent on the rate of loading, more so than in adults [3]. Increased thorax flexibility in younger occupants permits deformation to the underlying viscoelastic tissue, where a high loading rate results in lung injuries such as pulmonary contusion, without rib fracture. There have been pediatric biomechanical studies [4-6] aimed at characterizing the pediatric thoracic response in varying loading conditions including both distributed and belt loading that reported thorax compression magnitudes, thorax loads, and thorax compression rates along with injuries. This work has provided baseline information on pediatric thorax response and injury mechanisms to help guide child ATD development.

The National Highway Traffic Safety Administration (NHTSA) used this information, in part, to develop the Large Omni-directional Child (LODC) ATD. This ATD has been demonstrated to possess biofidelic thoracic response characteristics [7]. Using information from pediatric biomechanical studies, LODC thorax test data, and field injury

data, an injury risk function based on deflection rate has been proposed for the LODC [8] so that the ATD can be used to design optimized restraint strategies that mitigate thoracic trauma to children. To measure complex thoracic deformation, the LODC requires instrumentation that accurately tracks the distance between the compliant ribcage and flexible spine. Because of the ribcage and spinal compliance required to meet biofidelity criteria from pediatric studies, it would be ideal if the operation of deflection-measuring sensors is not affected by potentially extreme levels of deformation at the sensor connection points on the spine or ribcage. In early testing of the LODC with an IR-TRACC installed to measure chest deflection, because of the small LODC size, the IR-TRACC took up a large percentage of thoracic space and was prone to interference with the spine especially when the ribcage was loaded obliquely. This interference resulted in IR-TRACC damage or erroneous signals. Because of this, NHTSA initiated the development of an optical sensor system to measure deflection in the LODC ribcage [9]. This single laser sensor mounted to the thoracic spine was found to measure sternum deflections consistent with an IR-TRACC in controlled test setups.

Because initial bench testing of the single optical sensor in both static and dynamic modes was encouraging, full dummy testing was subsequently conducted to further evaluate the single sensor's performance. The LODC is intended to be tested in a variety of commonly used child restraint systems (CRS) as well as seating postures that do not use a CRS. The different test conditions will cause variations in the seat belt routing and will dramatically change the crash kinematics. The variation of the shoulder belt routing over the thorax means that a single sensor centered over the sternum may not detect maximum ribcage deflection if the belt doesn't cross in front of the sensor. A dramatic difference can be seen in the position of the shoulder belt relative to the ATD thorax when comparing the backless belt positioning booster (BPB) and the No CRS slouch test conditions (Figure 1). Figure 2 shows the internal chest deflection measured in these two seating conditions. When the shoulder belt crosses in front of the sensor measurement location on the ribcage with the booster, we see a higher deflection. When the shoulder belt crosses closer to the neck in the no booster case, the single deflection sensor located at the sternum understandably does not measure a similar result. However, from real-world cases, severe pneumothorax injuries can occur when the shoulder belt is not properly positioned on the chest [10]. This finding indicates that maximum ribcage deformation doesn't always occur mid-sternum in crashes and demonstrates the need to measure deflection at multiple locations on the ribcage.



**Figure 1. LODC seated on FMVSS No. 213 bench<sup>1</sup> with BPB (top) and slouch position without BPB (bottom).**

<sup>1</sup> FMVSS No. 213 bench shown is the proposed bench specified in the Notice of Proposed Rulemaking (NPRM). See <https://www.regulations.gov/search?filter=NHTSA-2020-0093-0004> for details of the bench.

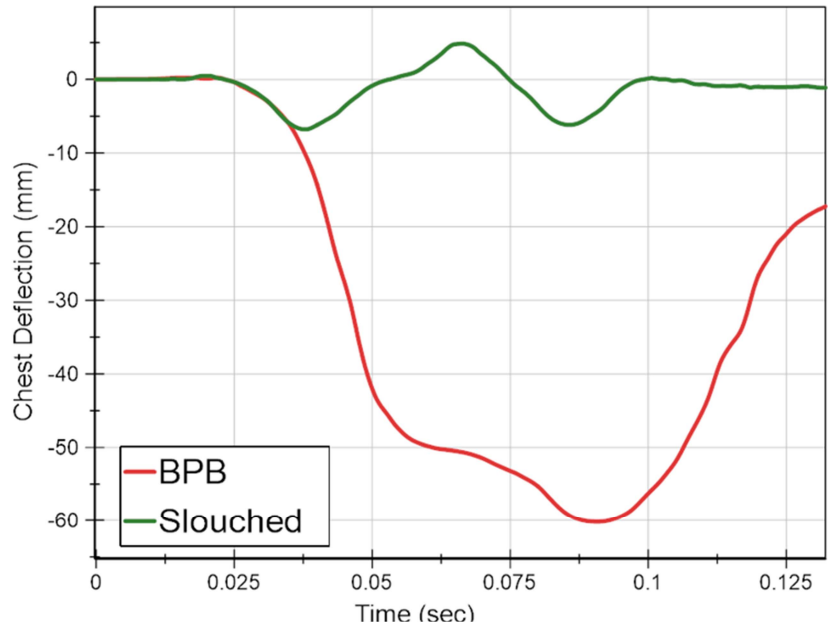


*Figure 2. Chest deflection as measured at the sternum of the LODC.*

#### DESCRIPTION OF MULTI-POINT LED SYSTEM

To facilitate measurement of deflection at multiple locations within the ribcage, a non-contacting optical sensor with a smaller footprint was required to fit into the LODC. The sensor chosen for this application is an off-the shelf optical triangulation distance sensor (Sensopart Model FT 25-RA-170-PNSUL\_M4M) that is commonly used in industrial applications (Figure 3). This particular sensor emits a beam of light that produces a spot on the inside of the ribcage. A lens focuses the spot image onto a photodiode that allows the calculation of the distance from the sensor to the spot (Figure 4). The optical triangulation sensor is limited by a standoff distance and a measurement range. The standoff distance is the closest distance in front of the sensor that will produce a measurement. The measurement range is the range of distance past the standoff distance that the sensor can measure. The chosen sensor specifications are expected to be able to measure the entire range of expected LODC ribcage deflection and motion.



*Figure 3. Sensopart distance sensor.*

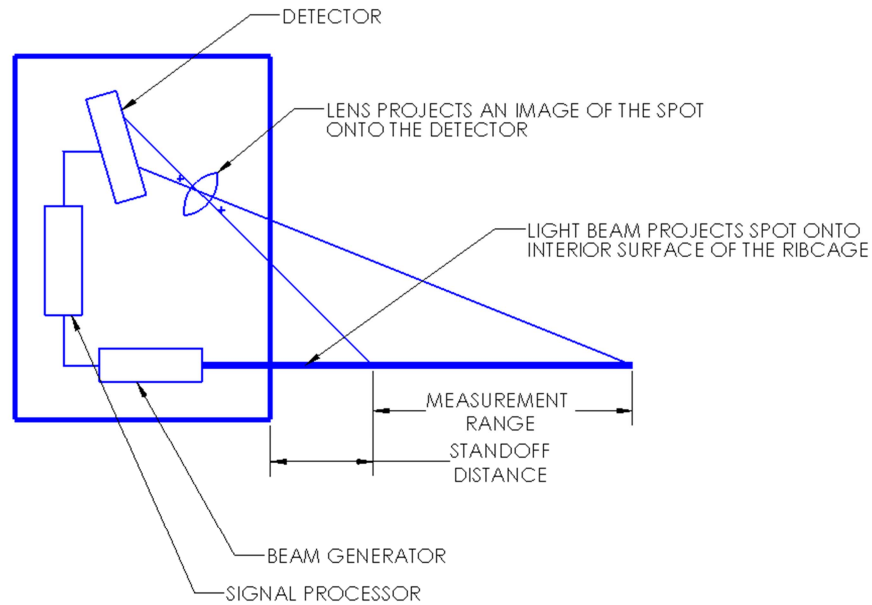


**Figure 4. Diagram of the optical triangulation distance sensor measurement.**

In the LODC, all seven sensors are attached to the center vertebrae element using brackets (Figure 5 and Figure 6). Five of the sensors face forward and two face obliquely. One sensor is located centered on the sternum between ribs 2 and 3. There are two forward facing sensors between ribs 1 and 2 and spaced laterally left and right of the midsagittal. There are two forward facing sensors between ribs 3 and 4 also spaced laterally left and right of the midsagittal. Finally, there are two sensors facing obliquely left and right between ribs 2 and 3 and rotated 70 degrees from the frontal direction. Figure 7 shows the system installed with LED spots visible on the inside surface of the ribcage.

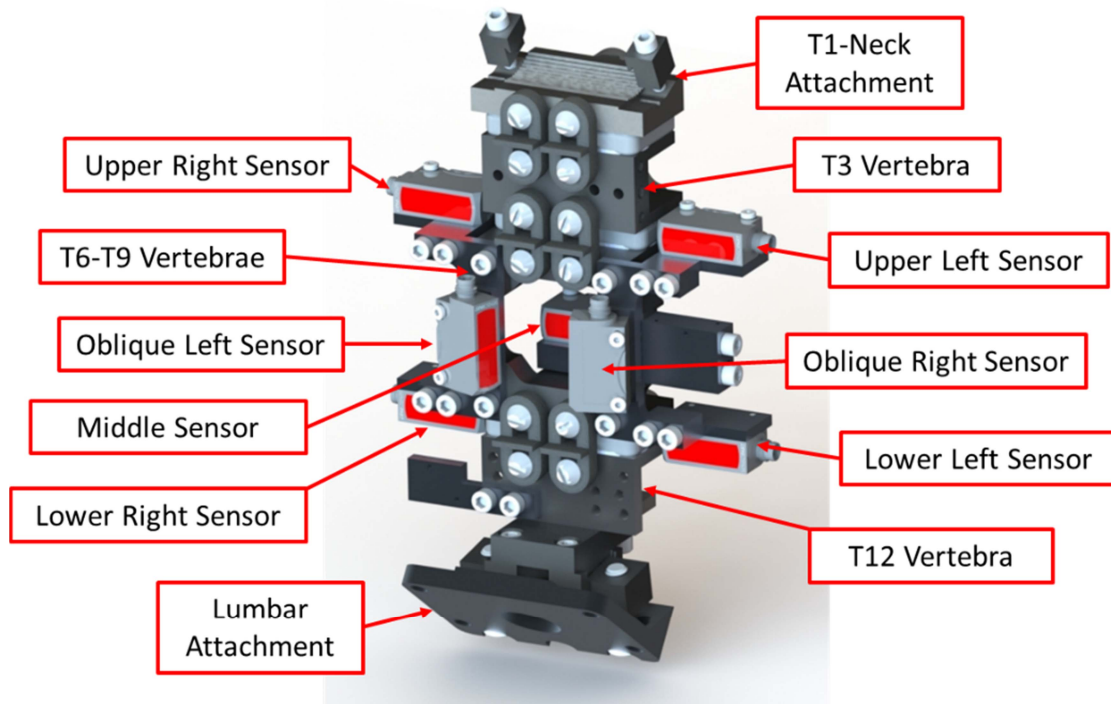


*Figure 5. LODC thoracic spine with the 7 optical sensors installed.*

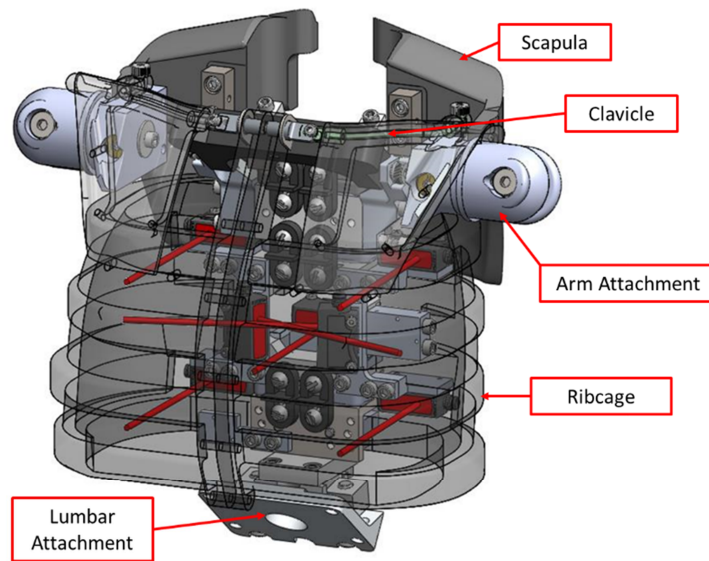


*Figure 6. Measurement locations of the optical sensors inside the LODC ribcage.*

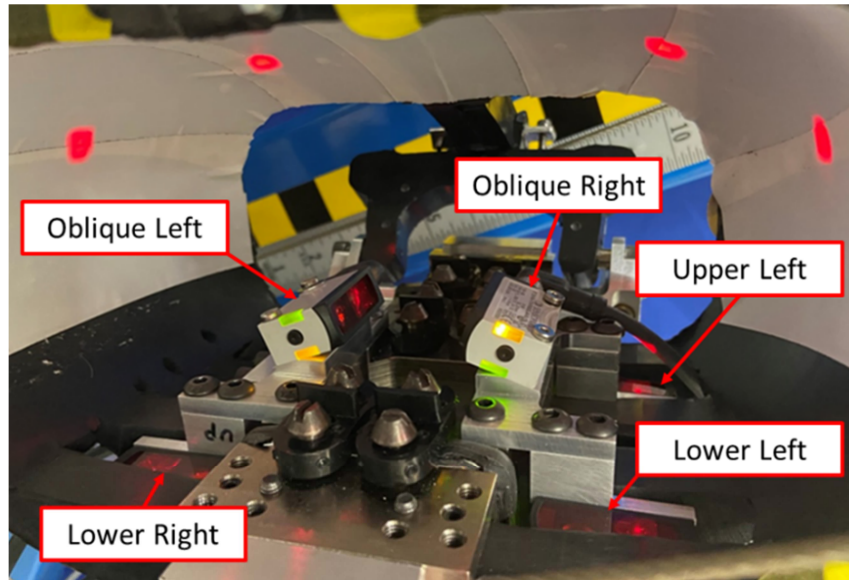


*Figure 7. Interior view (looking upwards) of ribcage showing sensors (upper right & midsternum not shown).*

Because of the difficulties associated with the IR-TRACC in the LODC, a triangulation sensor measurement system has been developed. The original optical system consisted of a single sensor located at the midsternum. After verifying proper operation of that system and recognizing the benefit of collecting chest deflection data at multiple locations in the ribcage, a multi-sensor configuration has been implemented into the LODC. The objective of this study is to evaluate the feasibility of a multi point sensing system in static, quasi-static and dynamic conditions.

#### **EVALUATION OF MULTI-POINT LED SYSTEM**

The multi-point chest deflection measurement system was evaluated in static, quasi-static, and dynamic conditions. Each sensor was first evaluated in a static calibration fixture prior to installation in the ribcage. The sensors were then evaluated quasi-statically through compression of the ribcage in a universal test machine (UTM). Thorax probe impacts and drop tower tests were performed to dynamically evaluate the multi-point system.

##### **Static Evaluation**

The calibration fixture consists of a linear slide connected to a linear scale with a digital readout. The sensor is clamped to the fixture as shown in Figure 8 and the slide is moved in 5 mm increments while the sensor reading is recorded.

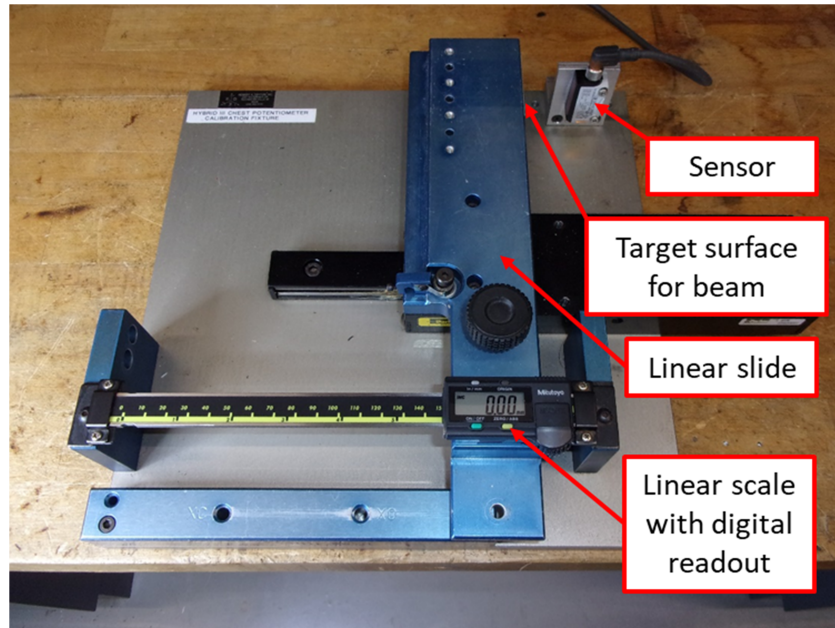


*Figure 8. Calibration fixture for static evaluation.*

A comparison of the linear scale readouts and sensor deflection readings are summarized in Table 1 for seven different sensors at each of the 5 mm increments. A plot of average sensor deflection versus linear scale deflection is shown in Figure 9.

**Table 1.**  
*Comparison of the linear scale readout and sensor deflection readings*

Linear Scale Readout	Deflection (mm)							Average
	#1	#2	#3	#4	#5	#6	#7	
0	0.0	0.0	0.0	0.0	0.0	0.0	0.0	0.0
5	5.1	5.1	5.3	5.5	5.2	5.5	5.2	5.3
10	10.1	10.1	10.4	10.3	10.2	10.7	10.2	10.3
15	15.1	15.1	15.3	15.4	15.2	15.6	15.3	15.3
20	20.0	20.2	20.4	20.5	20.1	20.6	20.3	20.3
25	25.1	25.2	25.5	25.5	25.4	25.6	25.4	25.4
30	30.1	30.2	30.3	30.4	30.2	30.6	30.3	30.3
35	35.1	35.1	35.3	35.5	35.2	35.5	35.3	35.3
40	40.0	40.2	40.3	40.3	40.2	40.6	40.2	40.3
45	44.9	45.2	45.3	45.4	45.3	45.5	45.2	45.3
50	50.0	50.2	50.3	50.5	50.3	50.6	50.3	50.3
55	55.0	55.2	55.2	55.3	55.2	55.5	55.2	55.2
60	60.0	60.1	60.3	60.4	60.2	60.5	60.1	60.2
65	65.0	65.0	65.1	65.5	65.2	65.7	65.3	65.3
70	70.0	70.0	70.2	70.4	70.2	70.5	70.2	70.2
75	75.1	75.1	75.2	75.4	75.1	75.4	75.2	75.2
80	80.1	80.1	80.4	80.2	80.1	80.5	80.2	80.2
85	85.1	85.0	85.5	85.3	85.3	85.4	85.1	85.2
90	90.0	90.1	90.7	90.4	90.1	90.5	90.2	90.3
95	95.1	95.2	94.9	95.3	95.2	95.4	95.3	95.2

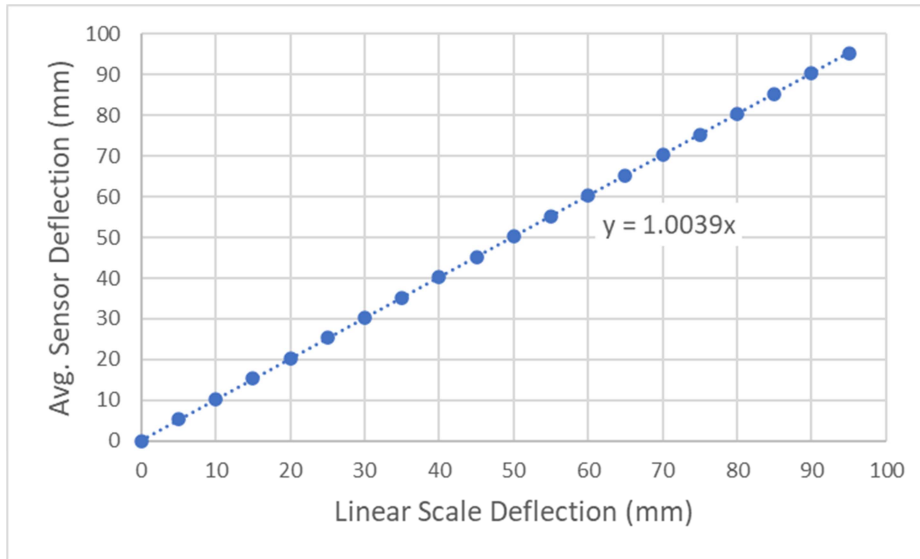


**Figure 9. Static evaluation – average sensor deflection versus linear scale deflection.**

The deflections as recorded by the sensors agree with the linear scale readings with an average difference of 0.268 mm over the 95 mm measurement range. Figure 9 indicates that over the full range, the sensor is on average 0.39% greater than the linear scale measurement.

### Quasi-static Evaluation

The quasi-static tests were performed using a United Testing Systems universal test machine (United UTM) to evaluate the accuracy of the sensors when integrated into the ribcage. The ribcage was assembled onto the thoracic spine and the spine was rigidly mounted in the United UTM so that the spine curvature was in the design position (as it would be in the assembled LODC). The mounting fixture was also designed to position the thorax such that the loading axis of the United UTM can be aligned with the primary axis of a particular sensor (Figure 10).

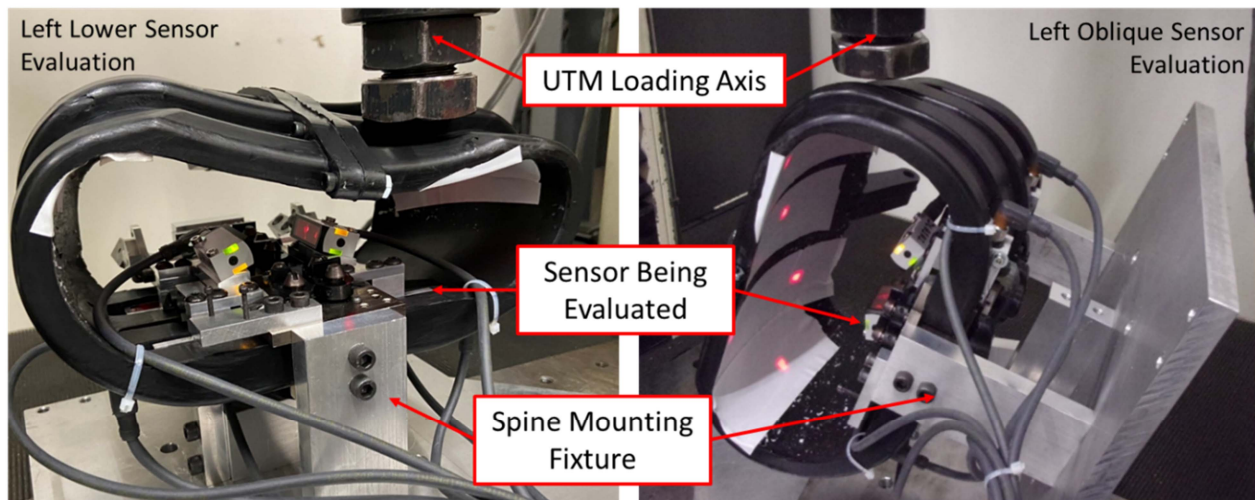


**Figure 10. Quasi-static testing of lower left sensor (left image) and left oblique sensor (right image).**

Each sensor was evaluated individually. The primary axis of the sensor being evaluated was aligned with the United UTM loading axis and the ribcage was then compressed to 10 mm, 20 mm and 30 mm. At each compression level, the sensor reading was recorded and a measurement of the sensor LED location on the inside surface of the ribcage was manually taken using a coordinate measuring machine (CMM) for comparison (Figure 11).

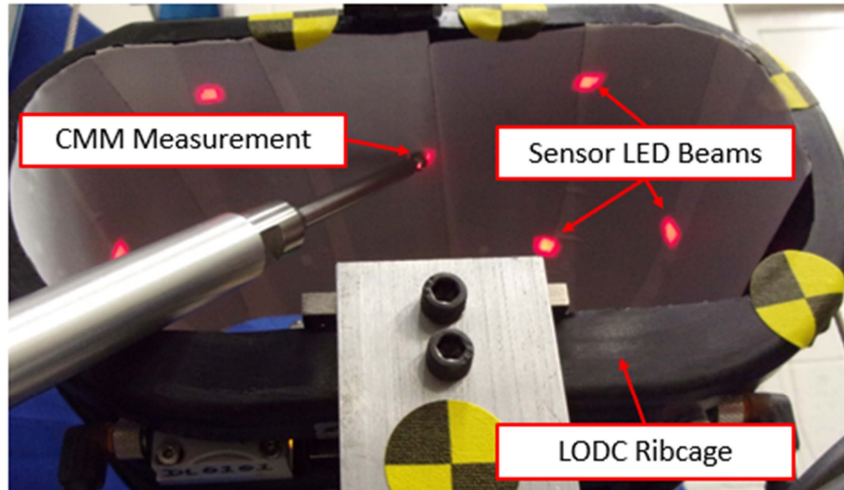


Figure 11. Sensor spot measurement using coordinate measuring probe.

Ribcage deflections at each of the United UTM compression levels were calculated from the sensor recordings and from the CMM measurements. Deflection results are summarized in Table 2.

Table 2.  
Ribcage deflections from sensor recordings and CMM measurements at each compression level

Sensor Location	United UTM Deflection (mm)	Average Deflection (mm)		Sensor-CMM Difference	
		Sensor	CMM	(mm)	%
Center	10	9.7	10.0	0.33	3%
	20	19.5	19.9	0.43	2%
	30	29.5	29.9	0.41	1%
Left Upper	10	8.9	9.0	0.10	1%
	20	17.9	18.4	0.55	3%
	30	27.0	27.7	0.65	2%
Left Lower	10	9.7	10.1	0.40	4%
	20	19.9	20.3	0.40	2%
	30	30.5	31.1	0.66	2%
Left Oblique	10	8.7	8.8	0.12	1%
	20	17.1	17.3	0.20	1%
	30	25.8	26.0	0.26	1%

The results show good agreement between the deflections as measured by the sensors and by the CMM with percent differences less than 5% at each of the sensor locations. In a controlled, quasi-static environment, the multi-point deflection sensors can accurately track the interior ribcage deflections.

### Dynamic Evaluation

**Probe Impacts** The LODC ribcage with the multi-point sensors installed was tested dynamically using a modified thorax qualification test setup. For this test the LODC was seated on a table with its flesh jacket, wetsuit, shoulders and arms removed. A fixed seatback was installed to prevent the LODC from sliding during the impact. Video captures from a test are shown in Figure 12. A probe impact to the LODC ribcage was performed at 4 m/s using the standard 6.99 kg LODC thorax qualification probe, which is equipped with an internally mounted accelerometer behind the front impact face. In addition to the multi-point deflection sensors, the LODC was also equipped with a T6 x-axis accelerometer to record motion of the spine during the test.

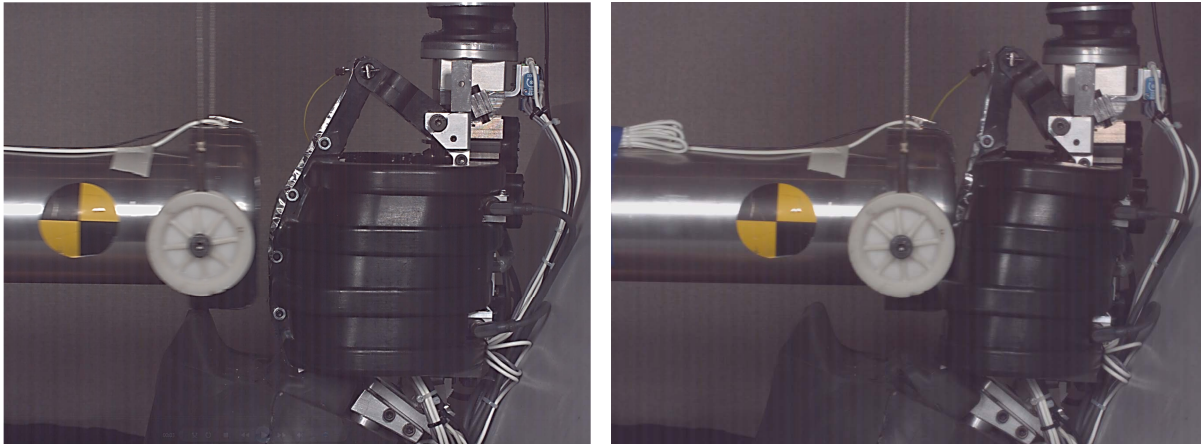


**Figure 12. Thorax probe impact. Right picture shows time of maximum ribcage compression.**

Internal ribcage deflections were calculated from each of the sensors during the impact event. Additionally, external ribcage deflection was calculated by subtracting the spine motion recorded by the T6-mounted accelerometer from the probe-mounted accelerometer and then double integrating that signal. Time histories of internal ribcage deflection as recorded by each of the sensors along with the calculated external deflection are shown in Figure 13. Unfortunately in this test, the right oblique sensor was not recorded as this sensor was out for calibration at the time of testing.

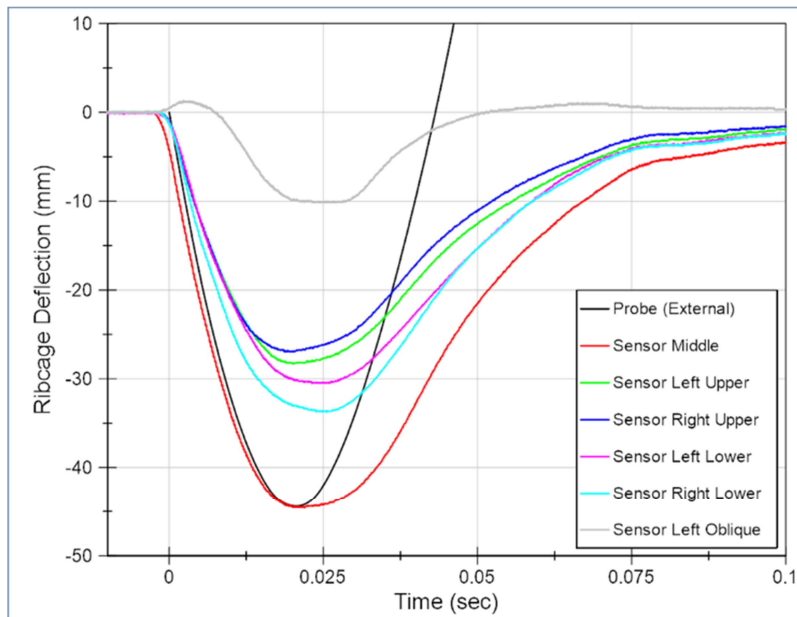


**Figure 13. Ribcage deflection-time histories during a dynamic probe impact. Internal ribcage deflections are measured by the multi-point sensors. External ribcage deflection is calculated from the impact probe.**

Although the LODC is not normally tested with a bare ribcage, dynamically impacting the LODC in this manner removes the effects of the flesh jacket and wetsuit to better evaluate the sensors. A direct impact to the ribcage can allow for the comparison of the internal deflection sensors with the external deflection as calculated by the impact probe. From the deflection-time histories in Figure 13, the midsternum or middle sensor deflection (red curve) shows good agreement with the calculated external deflection (black curve). The difference in duration between the probe-calculated deflection and the middle sensor is attributed to the test setup and calculation error in using the probe and T6 accelerations. Although a fixed seatback was used, soon after the ribcage reached maximum deflection, the thorax was observed to tilt backwards causing the probe and T6 mounted accelerometers to no longer

be in the same plane. This misalignment is why the calculated external deflection appears to rebound earlier than the ribcage sensors. The accelerometer from the probe can no longer track the actual ribcage position once the thorax begins to tilt, whereas the ribcage sensors can accurately track this position. This suggests that the sensors can accurately measure the internal deflection or motion of the ribcage throughout the loading phase of the event.

Additionally, the other internal deflection sensors were recorded (the right oblique sensor was not present) and show how the entire ribcage moves throughout the event. The midsternum or middle sensor (red curve) shows the largest deflection, which is understandable as this sensor is at the most forward part of the ribcage. The other four front-facing sensors (left and right lower, left and right upper) are grouped together with the lower sensors (magenta and cyan curves) showing slightly more deflection than the upper sensors (green and blue curves). The lower portion of the ribcage is unsupported unlike the upper portion of the ribcage, which is supported by a sternum bracket. The lack of support on the lower portion of the ribcage could explain the higher deflections of the lower sensors than the upper sensors. The left oblique sensor (grey curve) actually shows slight ribcage expansion (deflection in the positive direction) before compression. Although the right oblique sensor data was not available for this test (out for calibration), it can be expected to follow a similar pattern as the left oblique sensor since this impact was targeted at the center of the LODC.

An attempt was made to evaluate the LODC ribcage with the multi-point sensors in a similar test setup but in an oblique direction. However, it was difficult to prevent the motion of the thorax in this setup, so the ribcage with multi-point sensors was dynamically tested in the oblique direction using a drop tower instead.

**Drop Tower** The LODC ribcage with multi-point sensors was tested dynamically using a drop tower setup. The primary goal of this test condition was to examine how a full set of sensors would respond in an oblique loading scenario. The ribcage was mounted and positioned under a drop tower using the same mounting fixture used in the United UTM quasi-static test as shown in Figure 14.

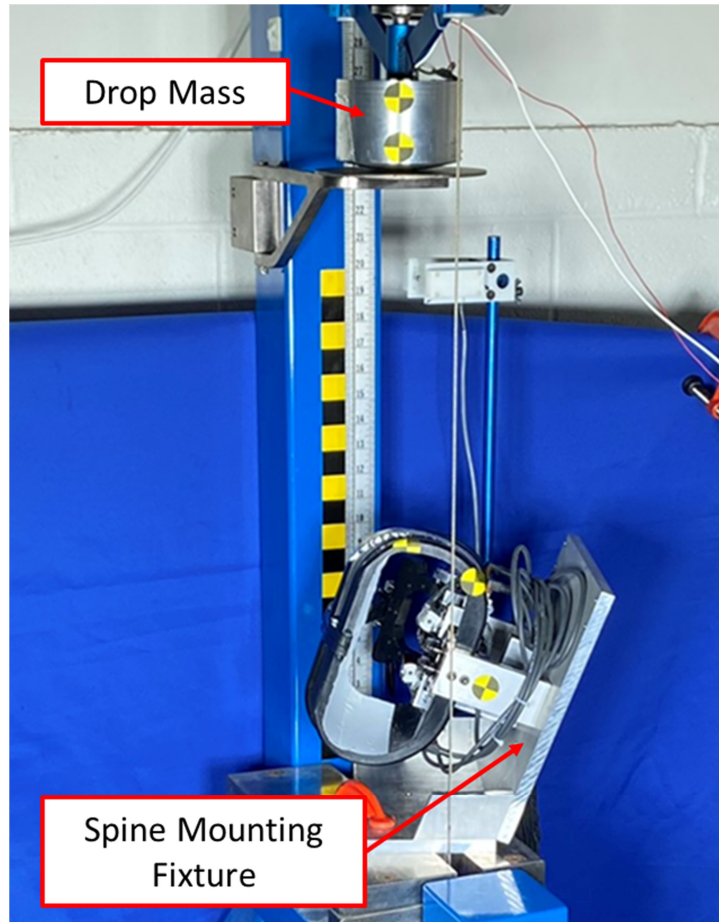


*Figure 14. Drop tower test setup for evaluating the left oblique sensor.*

Two tests were run using the drop tower as shown in Figure 15. For one test, a 1.86 kg mass was centered over the left oblique sensor and dropped at a velocity of 4 m/s. For the second test, the same mass was centered over the midsternum sensor and also dropped at a velocity of 4 m/s.

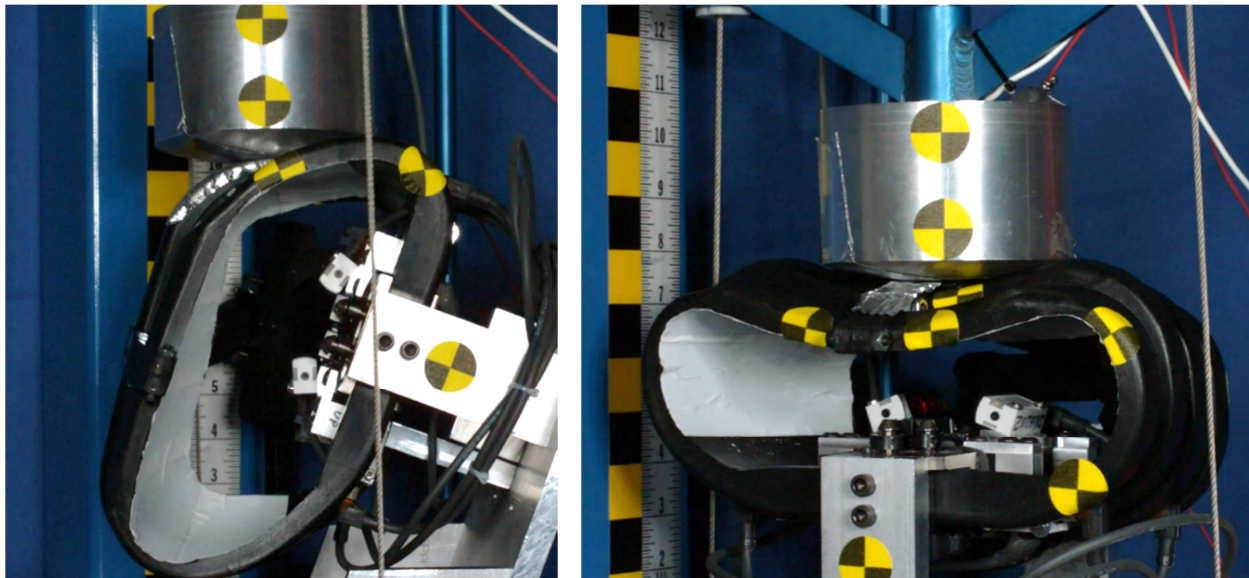


*Figure 15. Drop tower testing of the left oblique sensor (left image) and midsternum sensor (right image).*

Deflection-time histories for all sensors in the dynamic drop tower test aligned with the left oblique sensor are shown in Figure 16. As demonstrated earlier by the dynamic probe impact, this oblique drop tower test similarly shows how the entire ribcage moves and deflects throughout an oblique impact scenario. From the time history, there appear to be three groups of data traces. The left side of the ribcage was impacted in this test and the three left sensors (green, magenta and grey curves) show the greatest amount of deflection. The right front-facing (blue and cyan curves) and midsternum (red curve) sensors show the least amount of deflection and their data traces show slight ribcage expansion early in the event followed by ribcage compression. The right oblique sensor (orange curve), which was opposite of the impact side shows a large amount of ribcage expansion, which can also be observed in Figure 15 (left image).

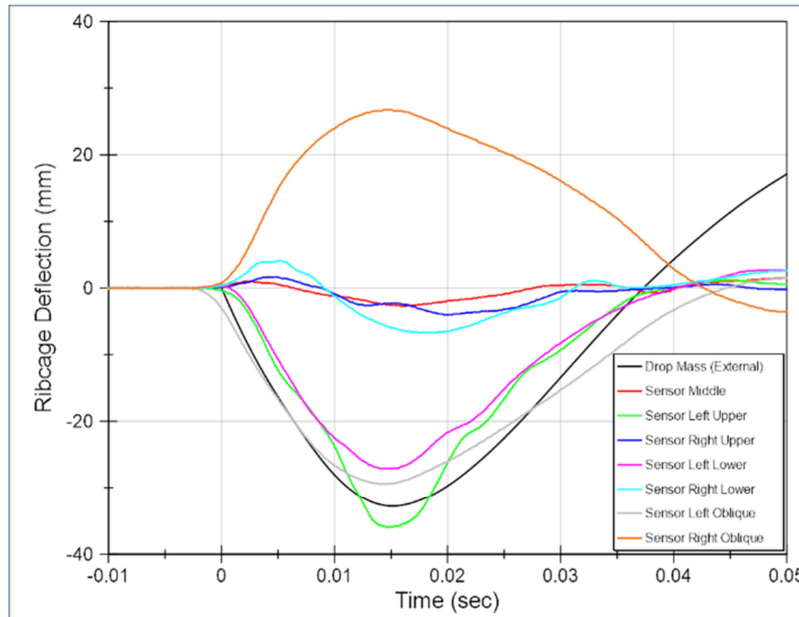


**Figure 16. Deflection-time histories for all sensors in the drop tower test aligned with left oblique sensor.**

Deflection-time histories for all sensors in the dynamic drop tower test aligned with the mid-sternum sensor are shown in Figure 17. The shape of the curves in this test are similar to those in the dynamic probe impact. The midsternum sensor (red curve) showed the greatest amount of deflection. The left lower (magenta curve) and right lower (cyan curve) sensors showed a greater amount of deflection than the left upper sensor (green curve), which is likely due to the lack of support at the bottom of the ribcage. The right upper sensor was out for calibration for this test, but it can be expected to follow a similar trend as the left upper sensor, as illustrated by the dynamic probe impact (Figure 13). The left oblique sensor (grey curve) and right oblique sensor (orange curve) similarly show the least amount of deflection and are characterized by ribcage expansion followed by compression, again similar to the dynamic probe impact.

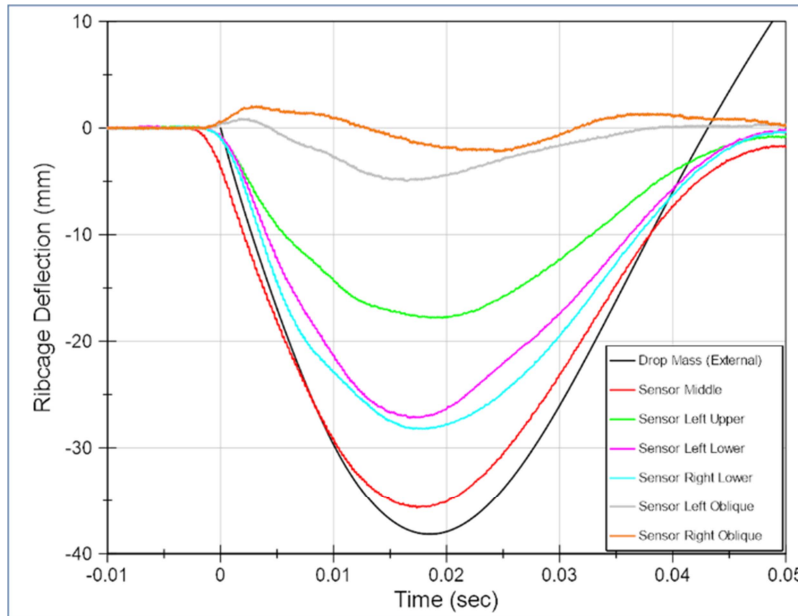


**Figure 17. Deflection-time histories for all sensors in the drop tower test aligned with midsternum sensor.**

The external drop mass deflections (black curves) show approximately 3-4 mm greater deflection than the sensors aligned with the impact: the left oblique sensor (grey curve in Figure 16) and the midsternum sensor (red curve in Figure 17). This is due to the rounded impact face of the drop mass used in this test. The rounded impact face allowed the drop mass to slide outward along the curvature of the ribcage and beyond peak ribcage deflection. This can be observed in Figure 15 (left image) where the centerline of the drop mass is no longer in line with the oblique sensor when the ribcage is at maximum deflection. As with the dynamic probe impact, the sensors were able to accurately measure the internal deflection and motion of the ribcage throughout the event.

Overall, the sensors performed well in dynamic impact scenarios as they agreed with externally measured deflections as well as provided a picture of how the ribcage deforms throughout a dynamic impact event.

## CONCLUSIONS

A novel non-contact sensor array to measure LODC chest deformation has been developed. This system has gone through a battery of both static and dynamic tests thus far to evaluate the system's performance. Individual sensors were found to be quite accurate in static verification tests, and sensors installed in the LODC ribcage were also observed to match well with CMM measurements. In dynamic testing with the full array of sensors installed in the ribcage, LED deflection matched probe-measured deflection closely. In both frontal and oblique drop tower tests, individual sensor deflection time histories showed how the full array could capture full ribcage deformation. This feature will be beneficial when the LODC is used in sled or crash testing. Future work will include more dynamic testing to further understand how the system can describe three-dimensional ribcage deformation.

## REFERENCES

- [1] Beck B, Bilston L, Kazzi M, Brown J. "Injury mechanisms in rear seated children aged 9-17 years and the implications for assessing rear seat protection in crash tests," *23<sup>rd</sup> Enhanced Safety of Vehicles Conference*, 2013, Paper No. 13-0392. Seoul, Korea.
- [2] Durbin D, et al. "Effects of seating position and appropriate restraint use on the risk of injury to children in motor vehicle crashes," *J Pediatrics*, 2005, 15:3.
- [3] Arbogast K, Locey C, Zonfrillo M. "Differences in thoracic injury causation patterns between seat belt restrained children and adults," *Annals of Advances in Automotive Medicine*, 2012, 56:213-221. Seattle, WA, USA.

- [4] Kent R, Lopez-Valdes F et al. "Characterization of the pediatric chest and abdomen using three post-mortem human subjects," 22<sup>nd</sup> *Enhanced Safety of Vehicles Conference*, 2011, Paper No. 11-0394. Washington, DC, USA.
- [5] Ouyang J, Zhao W, Xu Y, Chen W, Zhong S. "Thoracic impact testing of pediatric cadaveric subjects," *The Journal of Trauma*, 2006, 61(6):1492-1500.
- [6] Maltese M, Castner T et al. "Methods for determining pediatric thoracic force-deflection characteristics from cardiopulmonary resuscitation," *Stapp Car Crash Journal*, 2008, 52:83-105. San Antonio, TX, USA.
- [7] Stammen J, Suntay B, Moorhouse K, Carlson M, Kang YS. "The large omnidirectional child (LODC) ATD: Biofidelity comparison with the Hybrid III 10 year old," *Stapp Car Crash Journal*, 2016, 60:581-623. Washington, DC, USA.
- [8] Suntay B., Stammen J., Carlson M. "Abdominal and thoracic injury risk functions for the Large-Omnidirectional Child (LODC) ATD," Proceedings of the 2021 IRCOBI Conference, On-line, September 8-10, 2021.
- [9] Carlson M, Suntay B, Stammen J. "Development & evaluation of a new chest deflection measurement sensor for the Large Omnidirectional Child (LODC) ATD," *2020 SAE Government/Industry Meeting*.
- [10] García-España, J. and D. Durbin. "Injuries to belted older children in motor vehicle crashes," *Accident Analysis and Prevention*, 2008. 40(6): p. 2024-2028.